

Multiplex immunoassay analysis of biomarkers in clinically accessible quantities of human aqueous humor

Rajesh K. Sharma,¹ Anna T. Rogojina,² K.V. Chalam¹

¹Department of Ophthalmology, University of Florida, Jacksonville, FL; ²St. Jude Children's Research Hospital, Memphis, TN

Purpose: Aqueous humor is intimately related to the cells of the anterior and posterior chambers, which affect its composition. Aqueous analysis provides useful information regarding physiological and pathophysiological processes in the eye. Human aqueous samples are typically less than 100 μ l, limiting the usefulness of the analysis with traditional Enzyme-Linked Immunosorbent Assay (ELISA) techniques. The specific aim of this study was to investigate if whether large numbers of analytes can be identified in clinically available samples of aqueous humor and to document the detectability of certain biomarkers in the aqueous.

Methods: We used a technology developed by Luminex xMAP to analyze hundreds of analytes in a small sample. Aqueous from eight normal and two diabetic patients was analyzed.

Results: Of the 90 analytes evaluated, 52 (57%) were detectable in the normal aqueous. To place these results in biological context, we analyzed the list of expressed analytes using the MetaCore database. The functional pathways, networks, biological processes, and disease processes that these analytes represented were identified. Several ocular pathology-related processes were represented in the aqueous. The detected analytes represented biomarkers of several relevant disease processes including vascular diseases, arteriosclerosis, ischemia, necrosis, and inflammation. To provide the proof of principle that the aqueous profile could offer useful information about the pathophysiological processes, we analyzed two aqueous samples from diabetic patients. These limited samples showed the differences between normal and diabetic samples, including those relevant to diabetic retinopathy such as vascular endothelial growth factor (VEGF), C reactive protein, glutathione, and cytokines. Several biomarker groups for disease processes relevant to diabetes were perturbed.

Conclusions: These results demonstrate that multiplex analysis of the aqueous can be a useful tool in screening for any pathophysiological changes of the ocular environment. Moreover, ocular pathology/pathophysiology-specific Multi-analyte profiles MAPs can be developed and used to analyze the aqueous.

Aqueous humor, a product of the ciliary process, occupies the anterior and posterior chambers of the eye. It supplies nutrients to the nonvascularized cornea, lens, and trabecular meshwork. It is drained through two major pathways, the iridocorneal and the uveoscleral outflows. In turn, the constitution of aqueous humor affects the functioning of cells, and also the functioning of cells affects the aqueous composition. In addition, functional barriers between the anterior and posterior segments are not strict. The composition of the aqueous is also likely to be affected by the physiology/pathophysiology of the retina. Consequently, several growth factors have been detected in the aqueous humor, and the composition of these proteins changes dramatically in different ocular conditions, especially in inflammation and glaucoma [1,2].

Evaluation of the aqueous composition can be a powerful tool in understanding the pathophysiology and treatment response to many ocular conditions. Assessment of cytokines in uveitis patients revealed the presence of Interleukin (IL)-2,

6, 10, 12, Interferon (IFN)- γ , tumor growth factor (TGF)- β 2, tumor necrosis factor (TNF)- α , and macrophage migration inhibitory factor. One major limitation of testing the aqueous is that only small sample volumes can be obtained from human eyes. Typically 50-150 μ l of aqueous can be obtained from one human eye, which is barely sufficient to test a few cytokines using traditional ELISA techniques including sequential ELISA. Alternatively, the samples can be pooled, but this can mask individual patient differences. However, with the introduction of flow cytometric bead-based technology, multiple cytokine analytes can now be quantified simultaneously and rapidly in individual samples. This technique has better reproducibility and sensitivity than the traditional ELISA [3]. The cytometric bead array (CBA) system has proven effective in testing samples from cell culture supernatant, human serum, tears, and nasal lavage [4]. In this pilot study, we investigated the detectability of an array of proteins in the aqueous humor obtained from normal eyes to determine if this analysis could be useful in understanding disease processes and treatment responses within the eye.

The aim of this study was to investigate whether large numbers of analytes can be identified in clinically available aqueous samples. Large numbers of analytes are needed to

Correspondence to: Rajesh K. Sharma, M.D., Ph.D., Assistant Professor and Director of Research, Department of Ophthalmology, University of Florida, College of Medicine, Jacksonville, FL, 32209; Phone: (904) 244-9874; FAX: (904) 244-9391; email: rajesh.sharma@jax.ufl.edu

TABLE 1. LIST OF ANALYTES DETECTED IN AQUEOUS.

| Number | Analyte | SwissProt ID | Unit | Average | Standard deviation | Folds above detectable limits |
|--------|-----------------------------------|--------------|--------|---------|--------------------|-------------------------------|
| 1 | Alpha-1 Antitrypsin | P01009 | mg/ml | 0.00274 | 0.000893 | 52033.62 |
| 2 | Adiponectin | Q15848 | µg/ml | 0.01054 | 0.002623 | 10.545 |
| 3 | Alpha-2 Macroglobulin | P01023 | mg/ml | 0.0006 | 0.000777 | 2.07352 |
| 4 | Alpha-Fetoprotein | P02771 | ng/ml | 0.33637 | 0.072147 | 3.911337 |
| 5 | Apolipoprotein A1 | P02647 | µg/ml | 0.72 | 0.918 | 22077.51 |
| 6 | Apolipoprotein CIII | P02656 | µg/ml | 0.023 | 0.009896 | 1733.333 |
| 7 | Apolipoprotein H | P02749 | µg/ml | 0.61937 | 0.554624 | 14076.7 |
| 8 | Beta-2 Microglobulin | P61769 | µg/ml | 0.18121 | 0.126304 | 2745.644 |
| 9 | Complement 3 | P01024 | mg/ml | 0.00161 | 0.00162 | 61454.37 |
| 10 | Cancer Antigen 125 | Q14596 | U/ml | 9.83 | 11.01929 | 11.64692 |
| 11 | Cancer Antigen 19-9 | Q9BXJ9 | U/ml | 0.11567 | 0.048019 | 2.351045 |
| 12 | CD40 | P27512 | ng/ml | 0.03338 | 0.016927 | 7.949405 |
| 13 | C Reactive Protein | P02741 | µg/ml | 0.01163 | 0.011371 | 1520.686 |
| 14 | Endothelin-1 | P05305 | pg/ml | 3.867 | 1.675357 | 2.693245 |
| 15 | EN-RAGE | P80511 | ng/ml | 0.050 | | 10.06 |
| 16 | Eotaxin | P51671 | pg/ml | 11.737 | 3.148795 | 1.431402 |
| 17 | Erythropoietin | P01588 | pg/ml | 47.02 | 54.47922 | 1.416416 |
| 18 | Ferritin | P02792 | ng/ml | 3.10333 | 0.5231 | 443.3333 |
| 19 | FGF basic | P09038 | pg/ml | 20.66 | 5.233832 | 1.054082 |
| 20 | Fibrinogen | P02671 | mg/ml | 0.00021 | 0.000133 | 4374.364 |
| 21 | G-CSF | P09919 | pg/ml | 1.26 | | 1.26 |
| 22 | Glutathione S-Transferase | P09488 | ng/ml | 0.86112 | 0.971832 | 10.65749 |
| 23 | Haptoglobin | P00739 | µg/ml | 0.5 | 0.476 | 415.6686 |
| 24 | IgA | P24071 | µg/ml | 0.97 | 0.85 | 23278.44 |
| 25 | IGF-1 | P01343 | ng/ml | 3.7295 | 4.838829 | 4.661875 |
| 26 | IgM | P20769 | mg/ml | 4.82e-5 | 2.21e-5 | 638.4106 |
| 27 | IL-1ra | P18510 | pg/ml | 5.81 | | 1.936667 |
| 28 | IL-6 | P05231 | pg/ml | 5.81 | 7.328891 | 2.381148 |
| 29 | IL-8 | P10145 | pg/ml | 4.9412 | 2.029345 | 7.038818 |
| 30 | Leptin | P41159 | ng/ml | 0.11360 | 0.178015 | 5.514887 |
| 31 | Lipoprotein (a) | P08519 | µg/ml | 0.0637 | 0.043628 | 3.445946 |
| 32 | MCP-1 | P13500 | pg/ml | 308.87 | 191.7174 | 29.69952 |
| 33 | MIP-1alpha | P10147 | pg/ml | 7.1362 | 2.41117 | 2.744712 |
| 34 | MIP-1beta | P13236 | pg/ml | 21.707 | 13.95261 | 2.863786 |
| 35 | MMP-3 | P08254 | ng/ml | 0.22912 | 0.227617 | 5.728125 |
| 36 | Myoglobin | P02144 | ng/ml | 0.924 | 0.331162 | 176 |
| 37 | PAI-1 | P05121 | ng/ml | 0.62833 | 0.483399 | 139.6296 |
| 38 | Prostatic Acid Phosphatase | P15309 | ng/ml | 0.01419 | 0.00844 | 2.075815 |
| 39 | PAPP-A | Q13219 | U/ml | 0.01645 | 0.011151 | 2.223057 |
| 40 | "Prostate Specific Antigen, Free" | P07288 | ng/ml | 0.0051 | | 1.094421 |
| 41 | RANTES | P13501 | ng/ml | 0.00233 | 0.001534 | 9.668737 |
| 42 | Serum Amyloid P | P02743 | µg/ml | 0.0096 | 0.003076 | 841.7391 |
| 43 | Stem Cell Factor | P21583 | pg/ml | 20.575 | 4.99135 | 1.85027 |
| 44 | SGOT | P17174 | µg/ml | 1.0505 | 0.466578 | 1.411962 |
| 45 | SHBG | P04278 | nmol/l | 0.1696 | 0.070577 | 652.3077 |
| 46 | Thyroxine Binding Globulin | P05543 | µg/ml | 0.29598 | 0.26957 | 4339.993 |
| 47 | Tissue Factor | P13726 | ng/ml | 0.4732 | 0.156952 | 2.813615 |
| 48 | TIMP-1 | P01033 | ng/ml | 13.742 | 11.56826 | 327.5924 |
| 49 | TNF RII | Q92956 | ng/ml | 0.07006 | 0.051629 | 107.7949 |
| 50 | Thyroid Stimulating Hormone | P01215 | U/ml | 0.0217 | 0.018148 | 3.882143 |
| 51 | VCAM-1 | P19320 | ng/ml | 2.22 | 1.408971 | 170.7692 |
| 52 | VEGF | P15692 | pg/ml | 214.987 | 91.01978 | 143.325 |

Out of 90 analytes evaluated, 52 were detectable in the aqueous samples. These included cytokines, growth factors, cell adhesion molecules immunoglobulin, components of immune system, and enzymes. VEGF is especially relevant for studying the pathobiology of various retinal disorders.

perform global analysis for identifying maps, networks, pathways, and disease processes. Such an analysis would be useful to compare ocular environment in different conditions. Another aim of this study was to document the detectability of certain biomarkers in the aqueous.

METHODS

Samples: Aqueous samples were collected from eight non-diabetic and 2 diabetic patients undergoing cataract surgery. Aqueous humor (80–100 µl) was withdrawn through a limbal paracentesis site using a 27 gauge needle in a tuberculin syringe. Care was taken to avoid touching intraocular tissues and to prevent contamination of aqueous samples with blood. The samples were immediately frozen and stored at –80 °C.

TABLE 2. LIST OF 10 MOST SIGNIFICANT CANONICAL PATHWAYS MAPS REPRESENTED BY DETECTABLE ANALYTES IN NORMAL AQUEOUS SAMPLES.

| Number | Name | p value |
|--------|--|----------|
| 1 | Immune response_Histamine signaling in dendritic cells | 1.098e-7 |
| 2 | Development_Leptin signaling via JAK/STAT and MAPK cascades | 1.194e-7 |
| 3 | Immune response_Oncostatin M signaling via JAK-Stat in mouse cells | 1.335e-6 |
| 4 | Immune response_Oncostatin M signaling via JAK-Stat in human cells | 2.099e-6 |
| 5 | Immune response_Histamine H1 receptor signaling in immune response | 2.881e-6 |
| 6 | Cell adhesion_ECM remodeling | 3.911e-6 |
| 7 | Immune response_MIF-mediated glucocorticoid regulation | 1.501e-4 |
| 8 | Immune response_IL1 signaling pathway | 5.128e-4 |
| 9 | Immune response_Oncostatin M signaling via MAPK in mouse cells | 6.111e-4 |
| 10 | Immune response_Oncostatin M signaling via MAPK in human cells | 7.207e-4 |

These pathways prominently represent immune and cell adhesion pathways.

Patients with other ocular or systemic diseases such as inflammatory diseases were excluded from the study. Informed consent was obtained from the patients, and the research was in compliance with the tenets of the University of Florida and the Declaration of Helsinki for experiments involving human tissue.

Multiplex analysis: Multiplex analysis was performed at Rules-Based Medicine (Austin, TX), which uses Multi-Analyte Profiles (MAPs) based on powerful Luminex xMAP® technology to discover biomarker patterns within very small sample volumes. The aqueous samples were thawed at room temperature, vortexed, and then spun at 13,000x g for 5 min to remove any precipitates. Maximum available volume (80–100 µl) was removed and placed into a master microtiter plate for MAP antigen analysis. Using automated pipetting, an aliquot of each sample was introduced into one of the capture microsphere multiplexes of the human antigen MAP. The sample and capture microspheres were thoroughly mixed and incubated at room temperature for 1 h. Multiplexed cocktails of biotinylated reporter antibodies for each multiplex were then added robotically and thoroughly mixed. After this, the mixture was incubated for an additional hour at room temperature. Multiplexes were developed using an excess of streptavidin-phycoerythrin solution, which was thoroughly mixed into each multiplex and incubated for 1 h at room temperature. The volume of each multiplexed reaction was reduced by vacuum filtration, and the volume increased by dilution into a matrix buffer for analysis. Analysis was performed in a Luminex 100 instrument (Luminex, Austin, TX), and the resulting data stream was interpreted using proprietary data analysis software (developed at Rules-Based Medicine and licensed to Qiagen Instruments, Qiagen Inc., Valencia, CA). For each multiplex, calibrators and controls were both included on each microtiter plate. Eight-point calibrators were run in the first and last column of each plate, and three-level controls were included in duplicate. Testing results were first determined for the high, medium, and low controls of each multiplex to ensure proper assay performance. Unknown values for each of the analytes that localized in a specific multiplex were determined using

weighted and non-weighted curve fitting algorithms included in the data analysis package.

Analysis: The value for each analyte was obtained as a concentration (example; mg/ml). The values of eight samples (or less if an analyte could not be analyzed in all samples because of insufficient quantity of the sample) were averaged and compared to the sensitivity of the system. An analyte was considered “detectable” if the levels exceeded the minimal detectable levels.

The detectable analytes were further analyzed to identify biological/disease processes and the involved pathways/

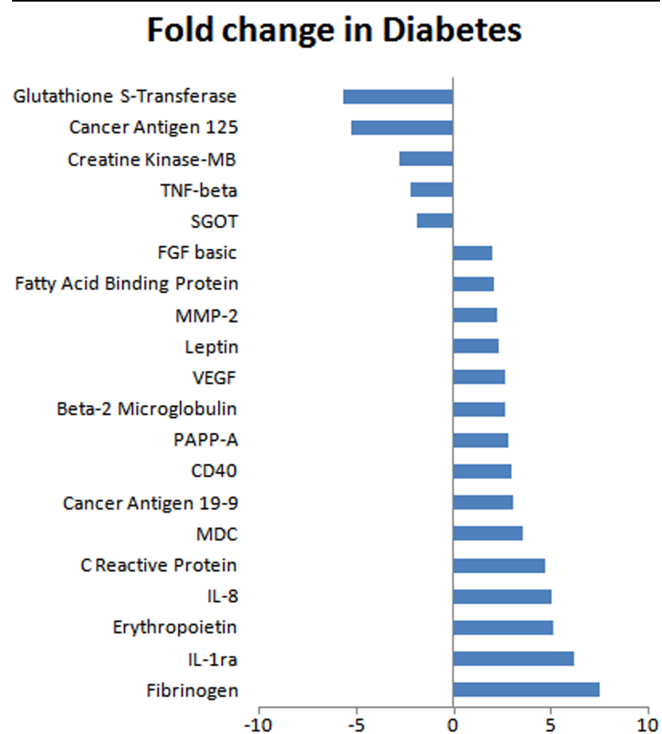


Figure 1. List of analytes that showed a twofold or more change in their levels in diabetic aqueous samples when compared to non-diabetic samples. The figure shows analytes that showed significant difference (2 fold or more; abscissa) between normal and the diabetic aqueous. The most prominent decrease was observed in glutathione S-transferase, and an increase in fibrinogen.

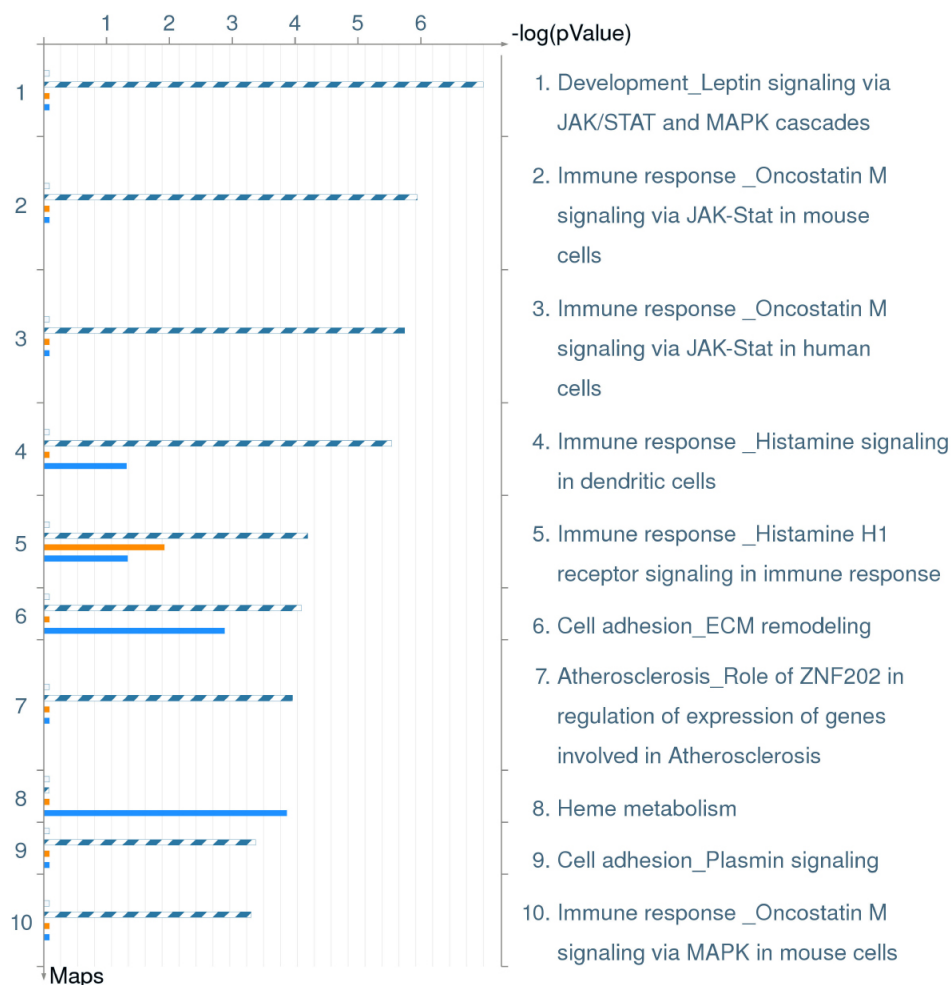


Figure 2. Distribution by canonical pathway maps in order of significance and their perturbation in diabetics. This figure shows canonical pathway maps, in order of significance and their perturbation in diabetics. Relevant to diabetes, the immune response and cell adhesion pathways were notably perturbed. Some pathways have been worked out in mouse cells and this is noted. The set of common analytes to both experiments is marked as blue/white stripes. The unique analytes are marked as colored bars (orange=diabetic, blue=normal/non-diabetic).

networks they participated in by using MetaCore™ analysis software (GeneGo Inc., St. Joseph, MI). The manually annotated database includes over 160,000 human protein interactions and metabolic reactions. The whole data set of 52 detectable analytes was imported in MetaCore to build an analysis of functional ontologies including GeneGo process, GeneGo disease process, canonical pathway maps, and networks. Calculation of statistical significance throughout MetaCore for maps, networks, and processes are based on p value, which are calculated based on hypergeometric distribution. P values essentially represent the probability of particular mapping arising by chance given the numbers of genes in the set of all genes on maps/networks/processes, genes on a particular map/network/process, and genes in the experiment [5]. We used a p value of 0.05 for the cutoff. The degree of relevance to different categories for the uploaded data sets is defined by p values, so that the lower p value obtains higher priority.

The experimental data were input to build networks. The three different scoring functions used to rank the small subnetworks created by the network building algorithms were zScore, gScore, and p value. The zScore ranks the

subnetworks (within the analyzed network) with regards to their saturation with genes from the experiment. A high zScore means the network is highly saturated with genes from the experiment. In other words, it means that relatively larger number of genes/analytes in a particular network were present in the aqueous sample. Each network is comprised of canonical pathways. The gScore modifies the zScore based on the number of canonical pathways used to build the network. If a network has a high gScore, it is saturated with expressed genes (from the zScore), and it contains many canonical pathways.

RESULTS

General analysis: A total of 90 predetermined analytes were analyzed. All 90 analytes could be analyzed in at least one sample from normal patients. In normal samples, 57% (52 out of 90) of the analytes were detectable (above the sensitivity of the method), and 42% of analytes (38 out of 90) were undetectable either because their values were below the sensitivity of the method (28 out of 90; 31%) or their quantities were insufficient to assign a value (10 out of 90; 11%). A list of detectable proteins is provided in Table 1.

TABLE 3. LIST OF 10 MOST STATISTICALLY SIGNIFICANT CANONICAL PATHWAYS MAPS REPRESENTED BY DETECTABLE ANALYTES IN NORMAL AQUEOUS SAMPLES.

| Number | Key network objects | GO Processes | p value | zScore | gScore |
|--------|---|---|----------|--------|--------|
| 1 | A2M, Kallikrein 3 (PSA), Alpha 1-antitrypsin, VEGF-A, PAII | organ development (61.4%; 4.075e-10), response to wounding (36.4%; 4.455e-10), response to external stimulus (43.2%; 4.572e-10), cell proliferation (50.0%; 5.309e-10), positive regulation of cell proliferation (31.8%; 6.986e-10) | 2.36e-31 | 61.1 | 61.1 |
| 2 | Stromelysin-1, CCL2, TIMP1, MIP-1-beta, Alpha 1-antitrypsin | response to external stimulus (47.8%; 1.468e-12), response to wounding (37.0%; 9.322e-11), wound healing (23.9%; 1.290e-10), blood coagulation (15.2%; 3.146e-07), coagulation (15.2%; 3.914e-07) | 8.46e-29 | 57.4 | 57.4 |
| 3 | VEGF-A, Endothelin-1, PAII, Stromelysin-1, CD40(TNFRSF5) | response to stimulus (75.5%; 5.440e-14), response to stress (55.1%; 3.472e-13), protein kinase cascade (40.8%; 3.739e-13), response to external stimulus (46.9%; 7.466e-13), cell surface receptor linked signal transduction (57.1%; 1.494e-12) | 1.14e-28 | 56.8 | 56.8 |
| 4 | F3, Beta-2-glycoprotein I (APOH), VCAM1, MIP-1-beta, CCL2 | cell adhesion (53.2%; 8.293e-19), biological adhesion (53.2%; 8.293e-19), response to wounding (51.1%; 1.218e-18), localization of cell (51.1%; 5.939e-17), cell motility (51.1%; 5.939e-17) | 1.14e-28 | 56.8 | 58.1 |
| 5 | CD40(TNFRSF5), CRP, G-CSF, F3, APCS | immune system process (57.1%; 2.349e-16), immune response (44.9%; 1.384e-14), response to stimulus (73.5%; 4.961e-13), defense response (40.8%; 6.493e-12), adaptive immune response (20.4%; 1.681e-10) | 1.14e-28 | 56.8 | 56.8 |
| 6 | APOA1, PPAP, Adiponectin, APOC3, MIP-1-alpha | sterol transport (15.2%; 3.842e-08), cholesterol transport (15.2%; 3.842e-08), triacylglycerol metabolic process (12.1%; 1.119e-06), lipid transport (15.2%; 1.661e-06), response to stimulus (63.6%; 1.781e-06) | 4.46e-27 | 57.2 | 57.2 |
| 7 | CCL2, CCL5, Eotaxin, MIP-1-beta, MIP-1-alpha | cytokine and chemokine mediated signaling pathway (25.5%; 4.692e-17), locomotory behavior (38.3%; 1.594e-16), chemotaxis (31.9%; 5.793e-16), taxis (31.9%; 5.793e-16), response to external stimulus (53.2%; 1.704e-15) | 1.82e-23 | 48 | 68 |
| 8 | A2M, Endothelin-1, CCL5, IL-6, MIP-1-beta | response to stimulus (75.5%; 5.440e-14), response to external stimulus (49.0%; 7.073e-14), regulation of protein metabolic process (34.7%; 5.809e-13), defense response (42.9%; 6.006e-13), inflammatory response (34.7%; 1.171e-12) | 5.95e-21 | 43.6 | 43.6 |
| 9 | Beta-2-microglobulin, APOA1, TR2(TNFRSF14), VCAM1, GSTM1 | response to stimulus (75.0%; 1.873e-11), positive regulation of transferase activity (27.5%; 2.304e-10), positive regulation of kinase activity (25.0%; 3.531e-09), positive regulation of catalytic activity (27.5%; 2.827e-08), regulation of transferase activity (27.5%; 3.249e-08) | 4.09e-16 | 34.9 | 34.9 |
| 10 | PPAP, Thyroxine-binding globulin, Adiponectin, Epo, APOLPA | protein kinase cascade (34.3%; 2.065e-07), intracellular signaling cascade (48.6%; 2.204e-07), positive regulation of kinase activity (22.9%; 2.930e-07), positive regulation of transferase activity (22.9%; 3.458e-07), regulation of cell differentiation (25.7%; 3.570e-07) | 2.29e-14 | 33.3 | 33.3 |

Network objects represent the fraction of the number of genes from input list against total number of genes from MetaCore database for respective network. These included cell adhesion pathways, cytokine signaling pathways, and pathways for immune system processes.

Functional analysis:

The detected analytes were evaluated by MetaCore software to identify possible relations among proteins. The accession numbers (SwissProt IDs) for the analytes in Table 1 were identified and uploaded into the MetaCore software. This software generates networks based on interactions between uploaded proteins and all others proteins/genes stored in the knowledge database. For each network, the probability of finding the uploaded proteins in the network by chance was calculated. The negative logarithm of the probability represents how relevant this network was to the list of uploaded proteins.

Distribution by canonical pathways maps

— Canonical pathway maps represent a set of approximately 500 signaling and metabolic maps covering human biology in a comprehensive way. Of the 52 proteins identified in the normal aqueous, 35 were present in the MetaCore database on maps. The 10 most significant canonical pathway maps that are represented relate to immune response, development, and cell adhesion (Table 2).

Most relevant networks—The list of detectable analytes was used to generate biological networks using the Analyze Networks (AN) algorithm, which is a variant of the shortest paths algorithm, with main parameters of (1) relative enrichment with the uploaded data and (2) relative saturation of networks with canonical pathways. Subnetworks are ranked by a p value and gScore and interpreted in terms of Gene Ontology. All 52 proteins identified were present in the MetaCore database on networks (Table 3).

Distribution by GeneGo and Gene Ontology processes

—The content of about 110 cellular and molecular processes is defined and annotated by GeneGo. Each process represents a preset network of protein interactions characteristic to the process. Of the 52 proteins identified, 41 were present in the MetaCore database on GeneGo processes. The top 10 processes represented in the normal aqueous samples are given in Table 4. These processes mostly represented responses to stimuli, immune processes, response to wounding, inflammation, defense and stress, cell proliferation, and chemotaxis.

Distribution by disease biomarkers

— There are over 500 human diseases with gene content annotated by GeneGo and organized in disease folders, which are further organized into a hierarchical tree. Certain factors may affect p value prioritization for diseases. For example, the gene content may vary greatly between complex diseases (such as cancers and some Mendelian diseases), and also, the coverage of different diseases in the literature may be skewed. Of the 52 proteins identified, 50 were present in the MetaCore database on diseases. The diseases whose biomarkers were detectable in the aqueous are relevant conditions of the retina including vascular (together with vascular occlusive and cardiovascular diseases), arteriosclerosis, ischemia, necrosis,

and inflammation. A list of top 10 disease processes represented is given in Table 5.

Comparison between non-diabetic and diabetic aqueous samples:

To provide the proof of principle that functional analysis of the aqueous using multiplex technology could provide useful information and identify differences between normal and disease conditions, we also performed the analysis on two diabetic samples. Out of 90 analytes, 44 (49%) were detected and 33 were not detected (36%). Quantity was not sufficient to analyze 13 analytes.

The comparison identified significant differences between the two groups with several analytes showing upregulation and downregulation. Analytes that showed twofold or more changes are shown in Figure 1. There were analytes uniquely expressed in diabetic or normal samples. Comparison between processes in non-diabetic and diabetic aqueous are shown in Table 6. There were also changes in the canonical pathways (Figure 2). The top 10 most significantly altered GeneGo processes included the ones that involved cell adhesion (platelet-endothelium leukocyte interactions, inflammation, chemotaxis, proliferation [positive regulation], and signal transduction; Figure 3). The vascular diseases, infarction, arterial occlusion, ischemia, arteriosclerosis, and

TABLE 4. LIST OF 10 MOST STATISTICALLY SIGNIFICANT GENE GO PROCESSES REPRESENTED BY DETECTABLE ANALYTES IN NORMAL AQUEOUS SAMPLES.

| Number | Process | p value |
|--------|---|----------|
| 1 | Response to external stimulus | 1.63e-11 |
| 2 | Response to stimulus | 2.9e-11 |
| 3 | Immune system process | 2.41e-9 |
| 4 | Response to wounding | 1.02e-8 |
| 5 | Inflammatory response | 1.04e-7 |
| 6 | Defense response | 1.36e-7 |
| 7 | Immune response | 3.86e-7 |
| 8 | Response to stress | 6.83e-7 |
| 9 | Positive regulation of cell proliferation | 7.37e-6 |
| 10 | Chemotaxis | 1.47e-5 |

Some of these processes, such as response to stress, chemotaxis, regulation of cell proliferation, wound healing, and immune system processes, are relevant in ocular diseases.

TABLE 5. LIST OF 10 MOST STATISTICALLY SIGNIFICANT DISEASE BIOMARKERS REPRESENTED BY DETECTABLE ANALYTES IN NORMAL AQUEOUS SAMPLES.

| Number | Name | p value |
|--------|-----------------------------|-----------|
| 1 | Vascular Diseases | 1.843e-21 |
| 2 | Arterial Occlusive Diseases | 5.575e-21 |
| 3 | Cardiovascular Diseases | 4.352e-20 |
| 4 | Arteriosclerosis | 5.866e-20 |
| 5 | Necrosis | 1.571e-18 |
| 6 | Ischemia | 9.303e-18 |
| 7 | Myocardial Ischemia | 1.746e-16 |
| 8 | Coronary Disease | 1.269e-15 |
| 9 | Infection | 1.637e-15 |
| 10 | Lung Diseases, Obstructive | 2.774e-15 |

Biomarkers for vascular diseases, ischemia, necrosis, and infection are highly relevant for ocular pathology.

TABLE 6. COMPARISON BETWEEN PROCESSES IN DIABETIC AND NON-DIABETIC AQUEOUS HUMOR.

| Number | Processes | Size | Target | Pathways | p value | zScore |
|------------------------------------|---|------|--------|----------|----------|--------|
| Common | | | | | | |
| 1 | Locomotory behavior (42.6%), G-protein coupled receptor protein signaling pathway (51.1%), cell surface receptor linked signal transduction (66.0%) | 50 | 13 | 10 | 8.58e-29 | 57.35 |
| 2 | Response to external stimulus (56.2%), response to wounding (47.9%), response to stimulus (79.2%) | 50 | 14 | 1 | 1.73e-31 | 61.78 |
| 3 | Lipid transport (29.4%), sterol transport (23.5%), cholesterol transport (23.5%) | 50 | 12 | 0 | 3.44e-27 | 57.78 |
| 4 | Immune system process (54.0%), organ development (68.0%), response to stimulus (74.0%) | 50 | 13 | 0 | 8.58e-29 | 57.35 |
| 5 | Response to stimulus (75.0%), response to wounding (40.9%), response to external stimulus (47.7%) | 50 | 7 | 6 | 4.60e-14 | 31.76 |
| Unique for Diabetes Samples | | | | | | |
| 1 | Response to external stimulus (50.0%), response to wounding (41.3%), cell surface receptor linked signal transduction (58.7%) | 50 | 4 | 0 | 1.33e-11 | 51.55 |
| 2 | Taxis (100.0%), chemotaxis (100.0%), locomotory behavior (100.0%) | 5 | 1 | 0 | 6.01e-04 | 40.77 |
| Unique for Normal Samples | | | | | | |
| 1 | Response to wounding (37.2%), response to stimulus (69.8%), intracellular signaling cascade (51.2%) | 50 | 8 | 0 | 1.68e-21 | 67.49 |
| 2 | Response to external stimulus (53.8%), response to wounding (46.2%), cell surface receptor linked signal transduction (64.1%) | 44 | 5 | 0 | 8.36e-13 | 44.93 |
| 3 | Cellular di-, tri-valent inorganic cation homeostasis (100.0%), di-, tri-valent inorganic cation homeostasis (100.0%), cellular cation homeostasis (100.0%) | 27 | 2 | 0 | 3.28e-06 | 37.72 |

The table lists the top related processes, the total number of genes in the network (Size), the number of genes in the network from the input list (Target) and the number of canonical pathways used to build the network (pathways). The comparison of diabetic and non-diabetic samples shows several processes listed under unique to diabetes and unique to normal samples changed in the diabetic and non-diabetic samples.

necrosis were the most significant diseases whose biomarkers were perturbed in diabetes (Figure 4).

DISCUSSION

MAPs are a fully developed and validated technique [6,7]. Rule based medicine's (RBM's) MAPs measure markers of cancer, infectious disease, autoimmunity, and cardiovascular risk (similar to age related macular degeneration [AMD] risk) as well as hormones, cytokines/chemokines, acute phase reactants, clotting proteins, growth factors, tissue modeling factors, and other typical plasma proteins [8]. A comprehensive analysis of an individual's physiological status can be obtained by measuring a broad spectrum of biomarkers using MAPs. Luminex technology performs up to 100 multiplexed, microsphere-based assays in a single reaction vessel by combining optical classification schemes, biochemical assays, flow cytometry, and advanced digital signal processing hardware and software.

Multiplex analysis has been performed on aqueous samples in the past but with smaller numbers of analytes [9, 10]. Our results demonstrate that with this technique around 100 different analytes can be successfully analyzed in small amounts of aqueous samples and provide base line values for 52 analytes. Many of the detected analytes such as CD40, C

reactive protein, endothelin, basic fibroblast growth factor (bFGF), fibrinogen, glutathione S-transferase, matrix metalloproteinase (MMP)-3, tissue inhibitors of metalloproteinases (TIMP)-1, and vascular endothelial growth factor (VEGF) are implicated in several ocular pathologies, and therefore, their measurement could provide useful information [11-14]. Degradation of extracellular matrix proteins is regulated by MMPs. The activity of MMPs is in turn regulated by their natural inhibitors, TIMPs. MMPs and TIMPs play an important role in the pathogenesis of neovascularization in the retina. It is suggested that an imbalance between MMPs and TIMPs leads to neovascularization by affecting levels of VEGF, one of several genes associated with angiogenesis [15,16]. The role of VEGF in retinal as well as iris neovascularization is well established, and anti-VEGF therapy is becoming standard in the management of retinal neovascularization.

The MAP that we used was not specifically designed for ocular conditions. However, a specifically designed MAP for investigating ocular disease processes such as response of treatment (e.g., intravitreal injection of bevacizumab or steroids) can provide valuable and relevant information. It can also provide a method for subclassifying/staging diseases based on the pathophysiological processes.

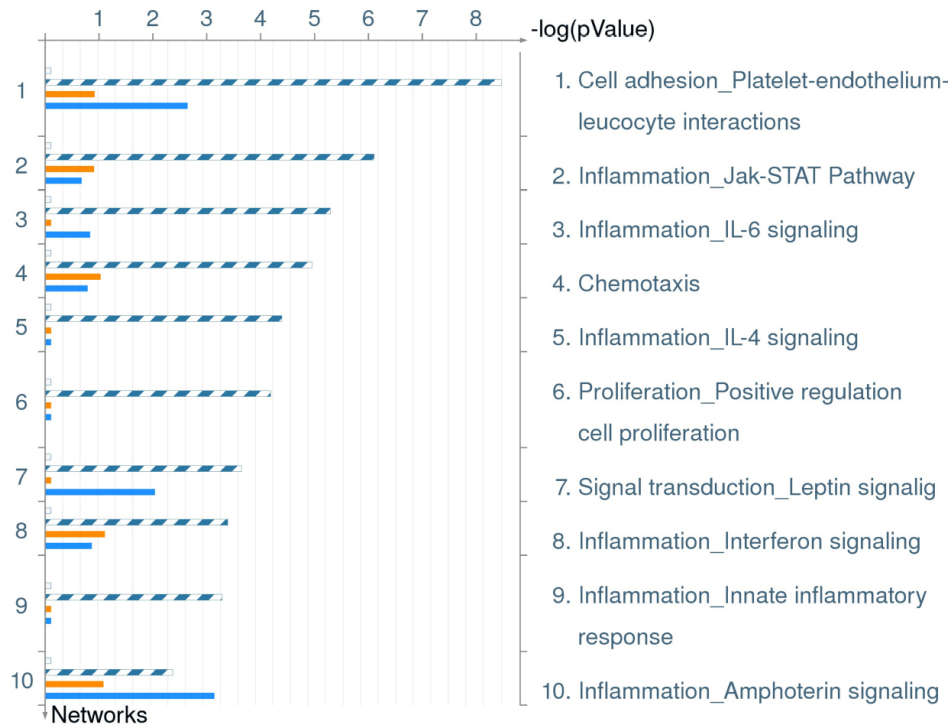


Figure 3. Distribution by GeneGo processes in order of significance and their perturbation in diabetics. This figure shows GeneGo processes in order of significance and their perturbation in diabetics. Relevant to diabetes, the cell adhesion, inflammation and chemotaxis pathways were notably perturbed. The set of common analytes to both experiments is marked as blue/white stripes. The unique analytes are marked as colored bars (orange=diabetic, blue=normal/non-diabetic).

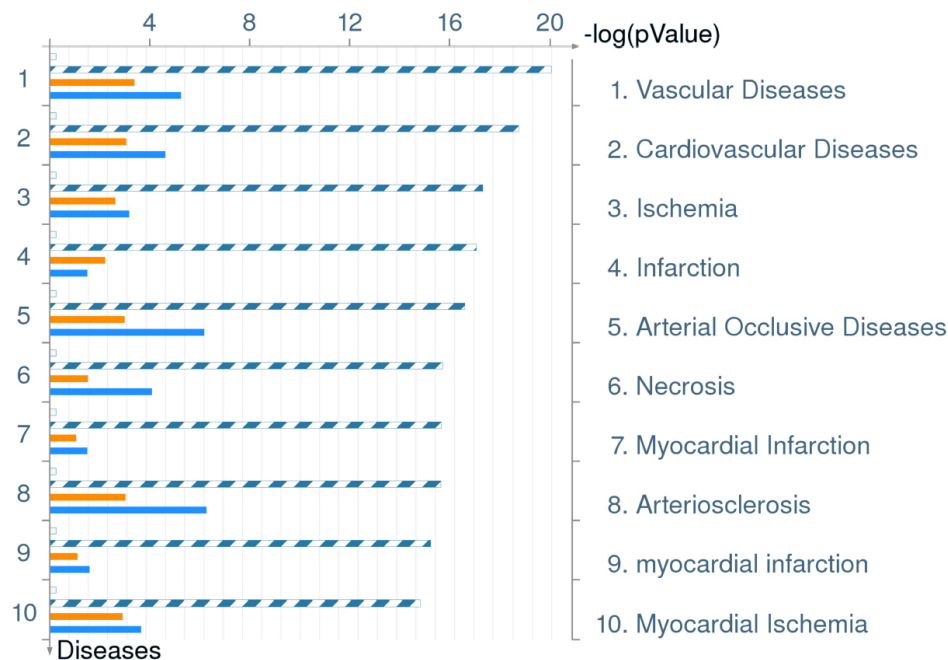


Figure 4. Distribution by disease biomarkers in order of significance and their perturbation in diabetics. This figure shows disease biomarkers in order of significance and their perturbation in diabetics. As expected in diabetes, biomarkers for vascular disease, ischemia and infarction showed perturbation. The set of common analytes to both experiments is marked as blue/white stripes. The unique analytes are marked as colored bars (orange=diabetic, blue=normal/non-diabetic).

We further analyzed the detected analytes to demonstrate the usefulness of global analysis in identifying cellular, biological, and disease processes to obtain an overall view of ocular physiology. Analytes represented a large number of pathways, albeit only a small number of proteins represented many of these. It should be noted that the MAP we used in this study did not represent all the cellular processes

uniformly. Therefore, our data does not indicate if any cellular process is more prevalent in aqueous than another. We also did not make any attempt to compare the extent of any cellular process represented in the MAP with that expressed in the aqueous. The results demonstrate that aqueous analysis can provide useful information about cellular and disease processes. One of the limitations of using Metacore™ or any

other similar program is that the output is not specific for ocular diseases. Output of our results included disease processes such as myocardial infarction and cardiovascular diseases. It is because the program outputs any disease processes where the input analytes participate. Therefore, these results should be interpreted in the context of ocular physiology. At a molecular level, aqueous analysis could identify the canonical pathways and the associated gene networks. The MAP used in this study did not include analytes uniformly across all the cellular/disease processes. Therefore, the data cannot be taken as a representation of these processes in physiological/pathological conditions. Nevertheless, our results demonstrate that the functional processes can be studied using this technology. Moreover, application of specific MAPs can be created to suit specific needs.

Another potential use of such an analysis could be comparing two samples for a global view of changes in the functional processes associated with the ocular environment. Such information may be useful in understanding the pathobiology of a disease, assessing progression of a disease, or response to a treatment. The analysis of diabetic samples provided proof of principle for this hypothesis. The aqueous from diabetic patients showed differences in expected and relevant cellular as well as disease processes. Some processes relevant to diabetic retinopathy were found upregulated in diabetic aqueous samples including CD40, C reactive protein, erythropoietin, fatty acid binding protein, FGF basic, fibrinogen, IL-1ra, IL-8, leptin, macrophage-derived chemokine (MDC), MMP-2, and VEGF [17,18]. Equally relevant for diabetic pathophysiology were creatine kinase-MB, glutathione S-transferase, SGOT, and TNF- β , and they were downregulated in the diabetic aqueous samples [19,20]. It should be noted that since only two diabetic samples were used, changes observed in specific analytes may not be conclusive. Larger sample sizes need to be compared to confirm conclusions. However, this study suggests multiplex analysis may be a valuable global screening technique to identify pathways that warrant further investigation.

ACKNOWLEDGMENTS

The authors wish to acknowledge the Dean's Grant Support, University of Florida, Jacksonville, FL.

REFERENCES

1. Welge-Lussen U, May CA, Neubauer AS, Priglinger S. Role of tissue growth factors in aqueous humor homeostasis. *Curr Opin Ophthalmol* 2001; 12:94-9. [PMID: 11224714]
2. Tripathi RC, Li J, Chan WF, Tripathi BJ. Aqueous humor in glaucomatous eyes contains an increased level of TGF-beta 2. *Exp Eye Res* 1994; 59:723-7. [PMID: 7698265]
3. van der Heyde HC, Burns JM, Weidanz WP, Horn J, Gramaglia I, Nolan JP. Analysis of antigen-specific antibodies and their isotypes in experimental malaria. *Cytometry A* 2007; 71:242-50. [PMID: 17252581]
4. Corrales RM, Villarreal A, Farley W, Stern ME, Li DQ, Pflugfelder SC. Strain-related cytokine profiles on the murine ocular surface in response to desiccating stress. *Cornea* 2007; 26:579-84. [PMID: 17525655]
5. Shipitsin M, Campbell LL, Argani P, Weremowicz S, Bloushtain-Qimron N, Yao J, Nikolskaya T, Serebryiskaya T, Beroukhim R, Hu M, Halushka MK, Sukumar S, Parker LM, Anderson KS, Harris LN, Garber JE, Richardson AL, Schnitt SJ, Nikolsky Y, Gelman RS, Polyak K. Molecular definition of breast tumor heterogeneity. *Cancer Cell* 2007; 11:259-73. [PMID: 17349583]
6. Toy D, Kugler D, Wolfson M, Vanden BT, Gurgel J, Derry J, Tocker J, Peschon J. Cutting edge: interleukin 17 signals through a heteromeric receptor complex. *J Immunol* 2006; 177:36-9. [PMID: 16785495]
7. Heuer JG, Zhang T, Zhao J, Ding C, Cramer M, Justen KL, Vonderfecht SL, Na S. Adoptive transfer of in vitro-stimulated CD4+CD25+ regulatory T cells increases bacterial clearance and improves survival in polymicrobial sepsis. *J Immunol* 2005; 174:7141-6. [PMID: 15905557]
8. Gurbel PA, Kreutz RP, Bliden KP, Dichiaro J, Tantry US. Biomarker analysis by fluorokine multianalyte profiling distinguishes patients requiring intervention from patients with long-term quiescent coronary artery disease: a potential approach to identify atherosclerotic disease progression. *Am Heart J* 2008; 155:56-61. [PMID: 18082490]
9. Ooi KG, Galatowicz G, Calder VL, Lightman SL. Cytokines and chemokines in uveitis: is there a correlation with clinical phenotype? *Clin Med Res* 2006; 4:294-309. [PMID: 17210978]
10. Ooi KG, Galatowicz G, Towler HM, Lightman SL, Calder VL. Multiplex cytokine detection versus ELISA for aqueous humor: IL-5, IL-10, and IFN-gamma profiles in uveitis. *Invest Ophthalmol Vis Sci* 2006; 47:272-7. [PMID: 16384973]
11. Symeonidis C, Diza E, Papakonstantinou E, Souliou E, Dimitrakos SA, Karakiulakis G. Correlation of the extent and duration of rhegmatogenous retinal detachment with the expression of matrix metalloproteinases in the vitreous. *Retina* 2007; 27:1279-85. [PMID: 18046238]
12. Laine M, Jarva H, Seitsonen S, Haapasalo K, Lehtinen MJ, Lindeman N, Anderson DH, Johnson PT, Jarvela I, Jokiranta TS, Hageman GS, Immonen I, Meri S. Y402H polymorphism of complement factor H affects binding affinity to C-reactive protein. *J Immunol* 2007; 178:3831-6. [PMID: 17339482]
13. Wang X, Baldrige WH, Chauhan BC. Acute endothelin-1 application induces reversible fast axonal transport blockade in adult rat optic nerve. *Invest Ophthalmol Vis Sci* 2008; 49:961-7. [PMID: 18326719]
14. Witmer AN, Vrensen GF, Van Noorden CJ, Schlingemann RO. Vascular endothelial growth factors and angiogenesis in eye disease. *Prog Retin Eye Res* 2003; 22:1-29. [PMID: 12597922]
15. Sharma RK, Johnson DA. Determinants of molecular mechanisms in neuroretinal development. In: Lajtha A, Johnson DA, editors. *Handbook of neurochemistry and molecular neurobiology: Sensory Neurochemistry*. 3rd ed. vol 20. New York: Springer; 2007.
16. Sharma RK. Molecular neurobiology of retinal degeneration. In: Lajtha A, Johnson DA, editors. *Handbook of neurochemistry and molecular neurobiology: Sensory Neurochemistry*. 3rd ed. vol 20. New York: Springer; 2007.

17. Simo R, Carrasco E, Garcia-Ramirez M, Hernandez C. Angiogenic and antiangiogenic factors in proliferative diabetic retinopathy. *Curr Diabetes Rev* 2006; 2:71-98. [PMID: 18220619]
18. Bulcao C, Ferreira SR, Giuffrida FM, Ribeiro-Filho FF. The new adipose tissue and adipocytokines. *Curr Diabetes Rev* 2006; 2:19-28. [PMID: 18220614]
19. Kim SK, Novak RF. The role of intracellular signaling in insulin-mediated regulation of drug metabolizing enzyme gene and protein expression. *Pharmacol Ther* 2007; 113:88-120. [PMID: 17097148]
20. Rabinovitch A. An update on cytokines in the pathogenesis of insulin-dependent diabetes mellitus. *Diabetes Metab Rev* 1998; 14:129-51. [PMID: 9679667]